Published in final edited form as:
Circ Cardiovasc Genet. 2010 February 1; 3(1): 78–87. doi:10.1161/CIRCGENETICS.109.871236.

Modulation of Mitochondrial Proteome and Improved Mitochondrial Function by Biventricular Pacing of Dyssynchronous Failing Hearts

Giulio Agnetti, PhD, **Nina Kaludercic, PhD**, **Lesley A. Kane, PhD**, **Steven T. Elliott, MS**, **Yurong Guo, PhD**, **Khalid Chakir, PhD**, **Daya Samantapudi, MD**, **Nazareno Paolocci, MD, PhD**, **Gordon F. Tomaselli, MD**, **David A. Kass, MD**, and **Jennifer E. Van Eyk, PhD**
Johns Hopkins Bayview Proteomics Center (G.A., L.A.K., S.T.E., J.E.V.E.), Baltimore, Md; INRC, Department of Biochemistry (G.A.), University of Bologna, Italy; Departments of Medicine (N.K., S.T.E., Y.G., K.C., D.S., N.P., G.F.T., D.A.K., J.E.V.E.) and Biological Chemistry (L.A.K., J.E.V.E.), Johns Hopkins University, Baltimore, Md; and Department of Clinical Medicine (N.P.), University of Perugia, Perugia, Italy.

Abstract

Background—Cardiac resynchronization therapy (CRT) improves chamber mechanoenergetics and morbidity and mortality of patients manifesting heart failure with ventricular dyssynchrony; however, little is known about the molecular changes underlying CRT benefits. We hypothesized that mitochondria may play an important role because of their involvement in energy production.

Methods and Results—Mitochondria isolated from the left ventricle in a canine model of dyssynchronous or resynchronized (CRT) heart failure were analyzed by a classical, gel-based, proteomic approach. Two-dimensional gel electrophoresis revealed that 31 mitochondrial proteins where changed when controlling the false discovery rate at 30%. Key enzymes in anaplerotic pathways, such as pyruvate carboxylation and branched-chain amino acid oxidation, were increased. These concerted changes, along with others, suggested that CRT may increase the pool of Krebs cycle intermediates and fuel oxidative phosphorylation. Nearly 50% of observed changes pertained to subunits of the respiratory chain. ATP synthase-β subunit of complex V was less degraded, and its phosphorylation modulated by CRT was associated with increased formation (2-fold, P=0.004) and specific activity (+20%, P=0.05) of the mature complex. The importance of these modifications was supported by coordinated changes in mitochondrial chaperones and proteases. CRT increased the mitochondrial respiratory control index with tightened coupling when isolated mitochondria were reexposed to substrates for both complex I (glutamate and malate) and complex II (succinate), an effect likely related to ATP synthase subunit modifications and complex quantity and activity.

Conclusions—CRT potently affects both the mitochondrial proteome and the performance associated with improved cardiac function.

Correspondence to Jennifer Van Eyk, PhD, The Hopkins Bayview Proteomics Center, 5200 Eastern Ave, Mason F Lord Building, Center Tower, Room 601, Baltimore, MD 21224. jvaneyk1@jhmi.edu.
Drs Kaludercic and Kane contributed equally to this work.

The online-only Data Supplement is available at http://circgenetics.ahajournals.org/cgi/content/full/CIRCGENETICS.109.871236/DC1.

Disclosures

Drs Van Eyk and Kass are consultants for Boston Scientific Research. Drs Kass and Tomaselli are recipients of funding from Boston Scientific Research.

Keywords

cardiac resynchronization therapy; mitochondria; proteomics; ATP synthase

Heart failure (HF) is a leading cause of morbidity and mortality in older adults, affecting 5 million individuals in the US alone.[1] A subset of patients with HF also develops regional conduction delay, resulting in discoordinate contraction that worsens symptoms and ultimate prognosis. Since the turn of the millennium, cardiac resynchronization therapy (CRT), also referred to as biventricular pacing, has become a clinical treatment for such patients, improving heart function, clinical symptoms, and survival.[2,3] Some recent studies[4–6] have revealed changes in gene expression and molecular remodeling of stress response kinases and cell survival signaling associated with CRT. Among the earliest findings in clinical CRT studies was the demonstration that CRT improves chamber energetic efficiency. This effect is rapid, resulting from the retiming of contraction to synchronously occur in both sides of the myocardium, reducing wasted chamber work much like tuning a car engine. Given the importance of abnormal mechanoenergetics in HF and centrality of ATP cycling,[7] we hypothesized that CRT may also modify the underlying mitochondrial machinery responsible for energy supply.

We determined protein changes in the mitochondrial subproteome by means of 2-dimensional gel-based (pH, 4 to 7 and 6 to 11) proteomics and additional detailed analysis of ATP synthase, the complex responsible for ATP production, using a recently developed and reported canine model of dyssynchronous heart failure and its resynchronization.[5] Our findings are consistent with cardiac resynchronization therapy acting as a metabolic therapy, increasing the abundance of enzymes that replenish the pool of Krebs cycle intermediates and reducing equivalents and subunits/mature complexes of the respiratory chain. We further demonstrate in dog's heart that cardiac resynchronization therapy modulation of a novel ATP synthase-β subunit phosphorylation (T311) may play a role in the regulation of complex V activity, protein turnover, and assembly.

Materials and Methods

Animal Model

Adult mongrel dogs (n=9) underwent either a dyssynchronous HF (DHF) or a CRT protocol, as previously described[8,9] (see the online Data Supplement for details).

Mitochondrial Fraction Preparation for Proteomics

The mitochondria-enriched fraction was prepared as we reported previously, with minor modifications.[10,11] A detailed protocol description is available in the Data Supplement.

Two-Dimensional Gel Electrophoresis

Two-dimensional gel electrophoresis (2DE) was performed on immobilized pH gradient 18-cm strips (GE Healthcare, Buckinghamshire, UK), pH ranges 4 to 7 and 6 to 11, in the first dimension (see the Data Supplement for details).

Protein Identification by Mass Spectrometry

Protein spots whose density was significantly changed with CRT were excised from fresh gels and digested as described previously.[12] Extracted peptides were submitted to tandem mass spectrometry (MS/MS; see the Data Supplement for details).

Phosphopeptide Analysis by Immobilized Metal Affinity Chromatography

Individual ATP-β spots separated by 2DE underwent in-gel trypsin digestion followed by extraction of the resulting peptides, as described in the Data Supplement. Phosphopeptides were enriched with an immobilized metal ion affinity chromatography column essentially as described by Ficarro et al,[13] with minor protocol modifications[12] described in the Data Supplement. The reported phosphopeptide sequence was confirmed by manual inspection of the MS/MS spectra.

ATP-β Dephosphorylation Assay

The phosphorylation status of ATP-β protein on 2DE gel was monitored using a modification of a previously described protocol[14,15] (see the Data Supplement for details).

Characterization of Isolated Complex V

Complex V was monitored by means of blue native-polyacrylamide gel electrophoresis (BN-PAGE) as described in detail in the Data Supplement. The presence of ATP-β in F_1/F_O complex was assayed through Western blotting using an anti-ATP-β antibody (MS503, Mitosciences, Eugene, Ore).

BN-PAGE gels also were used to measure the ATP synthase activity of complex V using the in-gel assay described by Bisetto et al[16] and as described in the Data Supplement.

Measurement of Oxygen Consumption in Isolated Mitochondria

Oxidative phosphorylation efficiency was measured on mitochondria freshly isolated from CRT and DHF animal hearts, as described previously.[17] Oxygen consumption was monitored at 37°C in the 2 groups in the presence of either glutamate/malate or succinate as substrates and after the addition of 300 μmol/L ADP or 10 μmol/L 2,4-dinitrophenol to induce state 3 and maximal respiration, respectively. Additional details are provided in the Data Supplemental Methods section.

2DE Data Analysis

Statistical significance of protein changes was assessed using 2-sided 2-sample *t* tests, assuming equal within-group variability. *P* and q values (for false discovery rate) are provided in the text and Table 2. All statistical analysis was performed using the open source statistical environment R (http://cran.r-project.org). After statistical analysis, a 1.5-fold cutoff was applied for biological significance[18] (see the Data Supplement for more details).

Results

CRT Improves Cardiac Chamber Function

As previously reported, both groups of animals developed dilated cardiomyopathy, with reduced ejection fractions and increased end-diastolic pressures. DHF hearts showed evidence of dyssynchrony (variance of peak systolic strain time around the heart 68±4.6 versus 31.3±5.1 in CRT [normal level is ≈30; $P<0.001$]). Animals assigned to CRT (biventricular pacing) had improved ejection fraction and contractility measured at week 6 when compared with those maintaining DHF (Table 1). Paired data between the third and sixth week time points have confirmed improved function in CRT and reduced function in DHF.[5] Table 1 summarizes functional data recorded from DHF and CRT animals before they were euthanized.

Protein Changes With CRT

Roughly 1200 protein spots were visible after silver staining on high-resolution 2DE gels in the 4 to 7 and 6 to 11 pH ranges (Figure 1). Thirty-one quantitative protein changes were observed in isolated mitochondria from CRT versus DHF hearts when controlling the false discovery rate at 30% (and 21 when controlling at 20% false discovery rate; see Table 2 for q values). Representative spot images and quantification of the various protein spots that changed between DHF and CRT are shown, clustered in functional groups, in Figure 2. Protein spot identifications, together with 2DE and MS/MS data, fold changes, and statistics, are listed in alphabetical order in Table 2 and numbered accordingly, together with the protein accession number as provided by National Center for Biotechnology Information nonredundant protein database ("other-mammals" subdatabase, see the Data Supplement for Table 2 description). Although 2DE is historically known for its bias against membrane proteins,[19] our optimized separation protocol[10] allowed us to obtain extensive representation of the mitochondrial proteome, including a large number of basic and membrane proteins (see Channels and Mitochondrial Membrane Proteins section).

Respiratory Chain

Approximately half of the observed mitochondrial protein changes (15 of 31) pertained to the respiratory chain, consistent with CRT modulating ATP production (Figure 2A). The changes were observed in all protein complexes of the respiratory chain, with the sole exception of complex IV, and included complex I 1α subcomplex 6, 14 kDa, Fe-S protein 1, 75 kDa, and B16.6, which were all increased (2- to 5-fold). The enzymatic complex linking the Krebs cycle to respiratory chain, complex II succinate dehydrogenase, increased in the CRT mitochondria (2-fold) and was phosphorylated (Supplemental Figure IA and IB), and 1 complex III subunit (binding protein) increased in CRT compared with DHF (3-fold). Interestingly, 2 different protein spots with different pI values were identified as cytochrome c (cytC); all of these exhibited a decrease in spot density in the biventricular pacing group (—2-fold,). Complex V also is changed, and given the importance of its modifications, we have characterized it in detail (see below).

Metabolic Pathways

Metabolic pathways that supply intermediates for the Krebs cycle (presented in Figure 2B) were all increased by CRT. The changes were observed in pyruvate carboxylase (3-fold) and pyruvate dehydrogenase, E1 (>10-fold) and E2 (2-fold) subunits. Additional key enzymes that fuel the Krebs cycle also were increased (Figure 2C) as follows: aldehyde dehydrogenase (2-fold), α-keto acid dehydrogenase E2 (2-fold), and ferredoxin reductase (2-fold). Fatty acid-binding protein, which participates in fatty acid transport into the mitochondrial matrix for final oxidation, also was increased by CRT (4-fold).

Protein Synthesis or Import

Proteins that participate in mitochondrial protein synthesis or import to mitochondria (Figure 2D) were mainly upregulated with one of the more prominent changes involving prohibitin 2 (5-fold). It is noteworthy that the prohibitin 2 protein spot (pI=10.04) is perfectly resolved, an uncommon observation for such an extremely basic protein. Leucine-rich PPR motif-containing protein also was increased (2-fold). The 28S mitochondrial ribosomal subunit (S22) declined in the CRT group (—1.5-fold).

Channels and Mitochondrial Membrane Proteins

Two isoforms of the voltage-dependent anion channels 2 and 3 showed a different abundance with CRT (—2-fold and 3-fold, respectively), indicating that the solubilization and separation methods used are effective in recovering and resolving very basic and

hydrophobic proteins (Figure 2E; also refer to Table 2 for predicted pI values). Additionally, a more acidic form of another mitochondrial membrane protein of unknown function, XP_533991, is recovered in the basic gels and decreased with CRT (—2-fold) (Figure 2F).

Reactive Oxygen Species Scavenging

The reactive oxygen species scavenging apparatus (Figure 2G) in the mitochondria was augmented by CRT, as reflected by increased levels of both thioredoxin-dependent peroxide reductase (>10-fold change) and a modified form (based on experimental pI deviation from the predicted one) of the programmed cell death 8 protein (apoptosis-inducing factor; 2-fold; Figure 2G). This and other protein changes (Figure 2H and 2I) are discussed in the Data Supplement (supplemental Results and Discussion sections).

Modifications of ATP Synthase

ATP-*β*, part of respiratory chain's complex V, was assigned to 6 protein spots. Because all of them displayed an experimental molecular weight (MW) lower than the theoretical one, they are likely the fragments of ATP-*β*. All were decreased (ranging from —3- to —2-fold; Figure 3A and supplemental Figure II). Because samples were kept on ice during mitochondrial enrichment and processed under identical conditions, it is unlikely that artifactual protein degradation occurred. Furthermore, mitochondrial samples left on ice for 8 hours (sampled every 2 hours) were subjected to 1DE separation and Western blot analysis, and no evidence of artifactual ATP-*β* protein degradation was discerned (data not shown).

To investigate the contribution of phosphorylation to ATP-*β* protein spot changes, we used a 2DE difference in-gel electrophoresis-based method in which endogenous samples (DHF and CRT) were pooled and dephosphorylated with alkaline phosphatase (AP) and used as an internal standard (dephosphorylated proteome). Figure 3B shows the 2DE separation of ATP-*β* obtained before and after dephosphorylation. The cluster of colored spots correspond to differently phosphorylated forms of ATP-*β* where based on CyDyes color assignment, the protein spots with a dominant red color (Cy3) are more abundant in DHF, and the spots with a dominant green color (Cy5) are more abundant in the CRT group. The blue channel (Cy2) detects the “dephosphorylated” proteome; hence, stronger blue color indicates less or unphosphorylated protein, confirming the presence of phosphorylation in adjacent acidic spots. Protein phosphorylation can affect electrophoretic mobility in 2 ways. The addition of a phosphate group not only can shift the pI of the protein toward the acidic end, but also can produce an apparent increase in the molecular weight by probably affecting protein-sodium dodecyl sulfate interaction (due to negative charge). Therefore, unphosphorylated (or less phosphorylated) ATP-*β* protein spots appear at the bottom right in Figure 3B compatible with a more basic pI and lower molecular weight after phosphate groups removal by AP. It is interesting to note that just a small fraction of the subunit is not phosphorylated (intact form; Figure 3, 2-fold increased, P=0.048, q=0.31), suggesting that very little of the subunit exists in an unmodified form in vivo and that post-translational modifications probably play a major role in regulating its biological function. We also found that another complex V subunit, ATP*δ*, was phosphorylated but similarly in both DHF and CRT (supplemental Figure IC and ID).

To characterize ATP-*β* protein phosphorylation in detail, immobilized metal ion affinity chromatography was used upstream of MS. MS/MS spectra of ATP-*β* peptide FT*QAGSEVSALLGR (m/z=709.4) is shown in Figure 3D. De novo sequencing confirmed the presence of a phosphate group based on b_{10} and b_{12} ions. The only phosphorylatable amino acid residue within this sequence is the threonine residue (T311). Interestingly, the

homolog position in rabbit sequence was found to be phosphorylated in rabbit heart on pharmacological preconditioning with adenosine.[12]

The complex assembly and degradation of ATP synthase is highly regulated. The effect of CRT on ATP-β protein inclusion into mature multimeric complexes (F_1/F_O) was monitored through BN-PAGE.[20] Mild detergent conditions, which still allowed separation of native complexes, were used in the electrophoretic separation. Figure 3C shows a Western blot analysis of a nondenaturing BN-PAGE gel where a specific antibody for ATP-β was used. The F_1/F_O of complex V was detected (a Western blot, using anti-ATP synthase-α subunit antibody, produced the same immunopattern; data not shown). The F_1 is membrane associated, whereas the F_O is the oligomycin-sensitive transmembrane portion; the F_1 classically consists of 3 α,3 β, and 2 δ subunits.[21] The intact F_1/F_O was increased in the CRT group (2-fold, P=0.004 versus CRT), indicating an increase of the mature, assembled complex V with CRT. Interestingly, the same form of the complex was not significantly changed in DHF compared with sham-operated animals (Figure 3C).

Mitochondria Coupling Improves With CRT

The efficiency of oxidative phosphorylation was determined in mitochondria isolated from shams and dogs subjected to DHF and CRT (Figure 4). In DHF dogs, mitochondrial oxygen consumption was significantly increased in the basal state (state 4) compared with shams or CRT in the presence of both complex I substrate glutamate/malate (Figure 4A) and complex II substrate succinate (Figure 4B). However, respiration in state 3 and uncoupled state, induced by addition of ADP and protonophore 2,4-dinitrophenol, respectively, did not differ between the groups. CRT prevented mitochondrial uncoupling, thus enhancing the respiratory control ratio over DHF (Figure 4C). ADP/oxygen ratio (Figure 4D), an index of the oxidative phosphorylation efficiency, was significantly greater in CRT and shams than in DHF mitochondria.

Finally, the intrinsic activity of complex V, isolated in native conditions according to Bisetto et al,[16] was increased by 20% with CRT compared with DHF (P=0.05; Figure 4E), whereas no significant difference was observed between DHF and sham animals. The activity was measured as the density of lead phosphate bands generated after incubation in the presence of ATP, normalized to the quantity of complex V (F_1/F_O), and, therefore, can be considered the “specific activity” of the complex (see also the Data Supplement).

Discussion

This study explored the mitochondrial subproteome of dys-synchronous and resynchronized (biventricular-paced) failing hearts, using an improved separation method for basic proteins,[10] a modified version of dephosphorylation 2DE (combining difference in-gel electrophoresis and AP treatment),[14] and a phosphopeptide enrichment MS-based method for phosphoresidues identification,[22] all of which were coupled with functional targeting of complex V. We identified 31 mitochondrial proteins and 2 mitochondria-associated proteins that were changed in the CRT group compared with DHF, controlling at 30% false discovery rate. These findings are summarized in a schematic shown in Figure 5. The changes encompass many facets of mitochondrial function, including metabolic pathways, ATP production, protein turnover, oxidative stress, and apoptosis. The results also were analyzed with the Ingenuity Pathways Analysis tool, which confirmed the significant regulation of mitochondrial dys-function and oxidative phosphorylation canonical pathways (supplemental Figure III).

The most important observation of our study is the modulation of metabolic pathways and ATP production machinery in CRT-treated hearts. Specifically, CRT seems to broadly

influence metabolic pathways that regulate pyruvate metabolism. Pyruvate carboxylase was notably increased with CRT. Pyruvate carboxylase is a key anaplerotic enzyme important for replenishing the Krebs cycle. Intracoronary administration of pyruvate to patients with HF acutely improves hemodynamics and cardiac performance, and this inotropic effect is thought to be mostly due to its effects on the Krebs cycle through pyruvate dehydrogenase and other anaplerotic pathways.[23] In the heart, the concentration of Krebs cycle intermediates is critical, and the depletion of carbon flux into the cycle results in contractile dysfunction.[24] It is likely that increased levels of pyruvate carboxylase provide a supplementary source of Krebs cycle intermediates. Carbon units traditionally enter the Krebs cycle through pyruvate dehydrogenase. The observed increase in the E1 and E2 subunits of pyruvate dehydrogenase likely underlies a parallel effect on the formation of Krebs cycle intermediate. Both pathways improve the use of pyruvate and the consequent formation of reducing equivalents (reduced nicotinamide-adenine dinucleotide and flavin-adenine dinucleotide, reduced form) that are later oxidized by the electron transport chain.

Another important metabolic pathway in the heart relates to branched-chain amino acid (Val, Leu, and Ile) oxidation because carbon derived from branched-chain amino acids also can replenish the Krebs cycle intermediates pool through the formation of acetyl-coenzyme A. Benefits from the use of branched-chain amino acids in isolated normal and septic hearts have long been recognized.[25,26] Intriguingly, we found that the E2 subunit of branched-chain α-keto acid dehydrogenase was increased in CRT compared with DHF. CRT also enhanced the abundance of fatty acid-binding protein, a well-established regulator of β oxidation, which fluctuates in mitochondria, along with peaks in β oxidative activity.[27] Heart metabolism in hypertrophic and failing hearts may shift from fatty acids to glucose utilization[28]; and in this light, an increase in fatty acid-binding protein might reflect the reversal to a more normal and efficient metabolic phenotype. This view also is supported by recent metabolomic studies. Turer et al[29] recently showed that ischemia/reperfusion injury decreases the oxidative fuel metabolism (fatty acids and ketone bodies) in favor of an increased glucose metabolism. Additionally, Mayr et al[30] recently analyzed the metabolomic and proteomic changes associated with human atrial fibrillation and found alterations of glycolytic enzymes in the absence of a significant increase of glucose metabolites. Further, the transcriptomic, proteomic, and metabolomic data pointed toward an inhibition of pyruvate dehydrogenase complex during atrial fibrillation, which agrees with our observations. Finally, the changes in metabolic proteins are supported by a recent transcriptomics study from our group.[6]

Succinate dehydrogenase was increased in CRT compared with DHF, suggesting that augmented availability of Krebs cycle intermediates may fuel the respiratory chain through complex II. While optimizing the ATP-β dephosphorylation assay, we also found that succinate dehydrogenase is heavily phosphorylated in this canine pacing model (supplemental Figure IA and IB). Moreover, the SDH protein spot increased with CRT (SSN 26) likely represents the un-phosphorylated, precursor form of the flavoprotein subunit of complex II, based on pI and MW co-ordinates. Therefore, the observed increase may be due to newly synthesized protein. The additional observation that isocitrate dehydrogenase activity is increased (supplemental Figure IV) provides functional evidence that Krebs cycle activity was stimulated with CRT.

More than half of the observed protein changes resided in the respiratory chain. Generally, subunits of complexes I, II, III, and V were increased on CRT, suggesting a compensatory shift toward an increased ability to produce ATP through oxidative phosphorylation. As such, it is surprising that 2 forms of cytC were decreased, and according to the difference between the observed and predicted pI and MW of the protein, these 2 forms likely represented modified forms of cytC. In this study, we were unable to observe a shift in the pI

of cytC after treatment with AP coupled with Western blot analysis, suggesting that (a) the observed pI shift is due to an unknown posttranslational modification; (b) cytC is phosphorylated, but the antibody used did not recognize this form of the protein; or (c) AP could not dephosphorylate cytC efficiently. Indeed, AP shows a low specificity by nature, and the assay conditions were optimized for ATP-β dephosphorylation; however, in general, the non-specificity of AP represents an advantage rather than a limitation, at least in broad-based screening dephosphorylation assays such as those required in proteomic analyses.[15]

The ATP-β subunit of complex V was less proteolyzed, and its phosphorylation status altered with CRT; the quantity of the mature F_1/F_O complex increased by 2-fold, and its specific activity increased by 20%, suggesting a novel mechanism for complex V activity regulation that acts both on complex V assembly and on specific activity. Indeed, CRT not only increases complex V assembly, but also is 20% more active. Interestingly, along with reduced degradation of ATP-β in CRT, prohibitin 2 increased. Prohibitin 2 is a chaperone known to regulate mitochondrial protein stability, and turnover and the deletion of prohibitin genes in yeast causes an increased degradation of mitochondrial membrane proteins by the membrane-embedded m-AAA protease system.[31] Augustin et al[32] reported the existence of a constant efflux of peptides derived from mitochondrial protein degradation into the cytosol and regulated by AAA-proteases and chaperones, such as the prohibitins. The authors estimated that more than half of these peptide species were derived from the electron transport chain proteins using MS/MS. The decrease of m-AAA proteases, such as ClpP with CRT, supports this view and suggests that ClpP is a potential candidate for the proteolysis of complex V observed in this study. When we performed a 2DE Western blot analysis for ClpP, we found 2 forms with the same pI but different MW ($\approx 10^3$ Da, supplemental Figure V). The higher MW form is reduced in agreement with our differential display analysis, whereas the lower MW form is increased with CRT.

This study also identified a novel phosphorylated amino acid residue of ATP-β isolated from the DHF heart (T311). T311 is homologous to a site previously identified by our group in the heart of rabbits subjected to adenosine-induced preconditioning.[12] We believe that this discovery is important because the site-specific characterization of posttranslational modification could help to identify candidate kinases and other enzymes based on their consensus sequence.

The functional role of this phosphorylation is unknown, and mutational studies to assess it are in progress, but it is tempting to speculate that phosphorylation may be involved in ATP synthase protein folding, activity, and turnover regulation. F_1/F_O complex assembly seems to be affected by phosphorylation mechanisms at least in yeast, where it has been extensively studied. These studies suggest that phosphorylation-induced conformational changes expose protease consensus sequences that normally would be buried in the unphosphorylated protein.[31] This view is in agreement with the increased formation of assembled F_1/F_O subunits with CRT, as shown by BN-PAGE in this study. The mechanism of assembly of complex V subunits into F_1 and F_O sectors is still the object of intense research, and a role for complex V modifications and assembly in mitochondrial uncoupling has been reported.[33] Yeast mutants lacking ATP-γ (γ-less yeast) grow very slowly on fermentable carbon sources, and this has been linked to a proton leak through complex V. In native conditions, the inhibitor protein (Inh1p) prevents ATP synthase from working in reverse as an ATPase. In γ-less yeast, Inh1p cannot efficiently bind complex V, and the complex dissipates protons and loosens mitochondrial coupling.[33] We report an increase in the respiratory control index, indicating a tighter mitochondrial coupling with CRT. This observation, together with the changes in ATP-β modifications and the improved activity and assembly of complex V with CRT, suggests that complex V is not only adapting, but also probably amplifying the beneficial effects of CRT on the upstream pyruvate

metabolism. Our group presently is investigating the causal relation between ATP-β modifications and complex V assembly and activity, which lies beyond the scope of this study. Moreover, the observation that the quantity and activity of mature complex V is not changed in DHF hearts compared with shams suggests that the beneficial effects of CRT rely on a compensatory response that involves energetics rather than a reversal to the sham phenotype.

Conclusions

We have shown that resynchronization by biventricular pacing of a dyssynchronous failing heart alters the expression and posttranslational status of many mitochondrial enzymes that fuel pyruvate metabolism and, therefore, the respiratory chain, the site of ATP production. Notably, we demonstrate that subunits of complex V (ATP synthase) are less degraded (ATP-β and -α) and differentially phosphorylated (ATP-β) with CRT. The specific activity and the quantity of mature complex V, as measured in native conditions, also are increased. These and other observed changes suggest that CRT acts at several coordinated levels of the mitochondrial proteome (the pyruvate metabolism, the Krebs cycle, the respiratory chain subunits) with targeted modifications and increased activity and assembly of complex V, resulting in the overall improvement of mitochondrial function. The data support the notion that in addition to enhancing mechanical efficiency at a chamber level, CRT potently alters cellular energy metabolism in the mitochondria, which may play an important role in the ability of CRT to enhance the systolic work performance of the failing heart acutely and chronically while also improving long-term survival—something not yet achieved by pharmacological therapies.

CLINICAL PERSPECTIVE

One of the limitations of cardiac resynchronization therapy is that 20 to 30% of the patients demonstrate little clinical benefit, if any at all. We believe that insight regarding the molecular mechanisms that are activated by cardiac resynchronization therapy may provide candidate targets that identify responders to this therapy and that proteomics could help in pinpointing the key proteins in this process and could narrow down the search for pathways that are dysregulated in nonresponders. Additionally, the study explores what the beneficial pathways activated by cardiac resynchronization therapy are in a well-established in vivo model.

Supplementary Material

Refer to Web version on PubMed Central for supplementary material.

Acknowledgments

Dr Brian O'Rourke (Johns Hopkins University) is acknowledged for the scientific discussion on XP_533991.

Sources of Funding

This study was supported by National Heart, Lung, and Blood Institute and National Institutes of Health P01HL081427 and P01HL077180 contracts (to J.E.V.E.) and grants PO1-HL077180 (to D.A.K. and G.F.T.); the Abraham and Virginia Weiss Professorship (to D.A.K.); the Michel Mirowski Professorship in Cardiology (to G.F.T.); the Compagnia di San Paolo, Turin, Italy (to G.A.); and the American Heart Association Mid Atlantic Post-doctoral fellowship (to N.K.).

References

1. Diwan A, Dorn GW II. Decompensation of cardiac hypertrophy: cellular mechanisms and novel therapeutic targets. Physiology (Bethesda) 2007;22:56–64. [PubMed: 17289931]
2. Spragg DD, Kass DA. Pathobiology of left ventricular dyssynchrony and resynchronization. Prog Cardiovasc Dis 2006;49:26–41. [PubMed: 16867848]
3. Bax JJ, Abraham T, Barold SS, Breithardt OA, Fung JW, Garrigue S, Gorcsan J III, Hayes DL, Kass DA, Knuuti J, Leclercq C, Linde C, Mark DB, Monaghan MJ, Nihoyannopoulos P, Schalij MJ, Stellbrink C, Yu CM. Cardiac resynchronization therapy: part 1—issues before device implantation. J Am Coll Cardiol 2005;46:2153–2167. [PubMed: 16360042]
4. Bilchick KC, Helm RH, Kass DA. Physiology of biventricular pacing. Curr Cardiol Rep 2007;9:358–365. [PubMed: 17877930]
5. Chakir K, Daya SK, Tunin RS, Helm RH, Byrne MJ, Dimaano VL, Lardo AC, Abraham TP, Tomaselli GF, Kass DA. Reversal of global apoptosis and regional stress kinase activation by cardiac resynchronization. Circulation 2008;117:1369–1377. [PubMed: 18316490]
6. Barth AS, Takeshi A, Halperin V, DiSilvestre D, Chakir K, Colantuoni C, Tunin RS, Dimaano VL, Yu W, Abraham PT, Kass DA, Tomaselli GF. Cardiac resynchronization therapy corrects dyssynchrony-induced regional gene expression changes on a genomic level. Circ Cardiovasc Genet 2009;2:371–378. [PubMed: 20031609]
7. Neubauer S. The failing heart—an engine out of fuel. N Engl J Med 2007;356:1140–1151. [PubMed: 17360992]
8. Spragg DD, Leclercq C, Loghmani M, Faris OP, Tunin RS, DiSilvestre D, McVeigh ER, Tomaselli GF, Kass DA. Regional alterations in protein expression in the dyssynchronous failing heart. Circulation 2003;108:929–932. [PubMed: 12925451]
9. Spragg DD, Akar FG, Helm RH, Tunin RS, Tomaselli GF, Kass DA. Abnormal conduction and repolarization in late-activated myocardium of dyssynchronously contracting hearts. Cardiovasc Res 2005;67:77–86. [PubMed: 15885674]
10. Kane LA, Yung CK, Agnetti G, Neverova I, Van Eyk JE. Optimization of paper bridge loading for 2-DE analysis in the basic pH region: application to the mitochondrial subproteome. Proteomics 2006;6:5683–5687. [PubMed: 17022103]
11. Kane LA, Neverova I, Van Eyk JE. Subfractionation of heart tissue: the “in sequence” myofilament protein extraction of myocardial tissue. Methods Mol Biol 2007;357:87–90. [PubMed: 17172681]
12. Arrell DK, Elliott ST, Kane LA, Guo Y, Ko YH, Pedersen PL, Robinson J, Murata M, Murphy AM, Marban E, Van Eyk JE. Proteomic analysis of pharmacological preconditioning: novel protein targets converge to mitochondrial metabolism pathways. Circ Res 2006;99:706–714. [PubMed: 16946135]
13. Ficarro SB, McCleland ML, Stukenberg PT, Burke DJ, Ross MM, Shabanowitz J, Hunt DF, White FM. Phosphoproteome analysis by mass spectrometry and its application to Saccharomyces cerevisiae. Nat Biotechnol 2002;20:301–305. [PubMed: 11875433]
14. Raggiaschi R, Lorenzetto C, Diodato E, Caricasole A, Gotta S, Terstappen GC. Detection of phosphorylation patterns in rat cortical neurons by combining phosphatase treatment and DIGE technology. Proteomics 2006;6:748–756. [PubMed: 16372257]
15. Matt P, Fu Z, Carrel T, Huso DL, Dirnhofer S, Lefkovits I, Zerkowski HR, Van Eyk JE. Proteomic alterations in heat shock protein 27 and identification of phosphoproteins in ascending aortic aneurysm associated with bicuspid and tricuspid aortic valve. J Mol Cell Cardiol 2007;43:792–801. [PubMed: 17949744]
16. Bisetto E, Di Pancrazio F, Simula MP, Mavelli I, Lippe G. Mammalian ATP synthase monomer versus dimer profiled by blue native PAGE and activity stain. Electrophoresis 2007;28:3178–3185. [PubMed: 17703470]
17. Bruzzone S, Dodoni G, Kaludercic N, Basile G, Millo E, De Flora A, Di Lisa F, Zocchi E. Mitochondrial dysfunction induced by a cytotoxic adenine dinucleotide produced by ADP-ribosyl cyclases from cADPR. J Biol Chem 2007;282:5045–5052. [PubMed: 17158448]

18. Blagoev B, Ong SE, Kratchmarova I, Mann M. Temporal analysis of phosphotyrosine-dependent signaling networks by quantitative proteomics. Nat Biotechnol 2004;22:1139–1145. [PubMed: 15314609]
19. Santoni V, Molloy M, Rabilloud T. Membrane proteins and proteomics: un amour impossible? Electrophoresis. 2000;21:1054–1070.
20. Schagger H, von Jagow G. Blue native electrophoresis for isolation of membrane protein complexes in enzymatically active form. Anal Biochem 1991;199:223–231. [PubMed: 1812789]
21. Oster G, Wang H. Reverse engineering a protein: the mechanochemistry of ATP synthase. Biochim Biophys Acta 2000;1458:482–510. [PubMed: 10838060]
22. Agnetti G, Kane LA, Guarnieri C, Caldarera CM, Van Eyk JE. Proteomic technologies in the study of kinases: novel tools for the investigation of PKC in the heart. Pharmacol Res 2007;55:511–522. [PubMed: 17548206]
23. Russell RR III, Taegtmeyer H. Pyruvate carboxylation prevents the decline in contractile function of rat hearts oxidizing acetoacetate. Am J Physiol 1991;261:H1756–H1762. [PubMed: 1750532]
24. Gibala MJ, Young ME, Taegtmeyer H. Anaplerosis of the citric acid cycle: role in energy metabolism of heart and skeletal muscle. Acta Physiol Scand 2000;168:657–665. [PubMed: 10759602]
25. Markovitz LJ, Hasin Y, Dann EJ, Gotsman MS, Freund HR. The different effects of leucine, isoleucine, and valine on systolic properties of the normal and septic isolated rat heart. J Surg Res 1985;38:231–236. [PubMed: 3982017]
26. Ichihara K, Neely JR, Siehl DL, Morgan HE. Utilization of leucine by working rat heart. Am J Physiol 1980;239:E430–E436. [PubMed: 6778220]
27. Fournier NC, Rahim M. Control of energy production in the heart: a new function for fatty acid binding protein. Biochemistry 1985;24:2387–2396. [PubMed: 3995017]
28. Glatz JF, Bonen A, Ouwens DM, Luiken JJ. Regulation of sarcolemmal transport of substrates in the healthy and diseased heart. Cardiovasc Drugs Ther 2006;20:471–476. [PubMed: 17119873]
29. Turer AT, Stevens RD, Bain JR, Muehlbauer MJ, van der Westhuizen J, Mathew JP, Schwinn DA, Glower DD, Newgard CB, Podgoreanu MV. Metabolomic profiling reveals distinct patterns of myocardial substrate use in humans with coronary artery disease or left ventricular dysfunction during surgical ischemia/reperfusion. Circulation 2009;119:1736–1746. [PubMed: 19307475]
30. Mayr M, Yusuf S, Weir G, Chung YL, Mayr U, Yin X, Ladroue C, Madhu B, Roberts N, De Souza A, Fredericks S, Stubbs M, Griffiths JR, Jahangiri M, Xu Q, Camm AJ. Combined metabolomic and proteomic analysis of human atrial fibrillation. J Am Coll Cardiol 2008;51:585–594. [PubMed: 18237690]
31. Arnold I, Langer T. Membrane protein degradation by AAA proteases in mitochondria. Biochim Biophys Acta 2002;1592:89–96. [PubMed: 12191771]
32. Augustin S, Nolden M, Muller S, Hardt O, Arnold I, Langer T. Characterization of peptides released from mitochondria: evidence for constant proteolysis and peptide efflux. J Biol Chem 2005;280:2691–2699. [PubMed: 15556950]
33. Ackerman SH, Tzagoloff A. Function, structure, and biogenesis of mitochondrial ATP synthase. Prog Nucleic Acid Res Mol Biol 2005;80:95–133. [PubMed: 16164973]

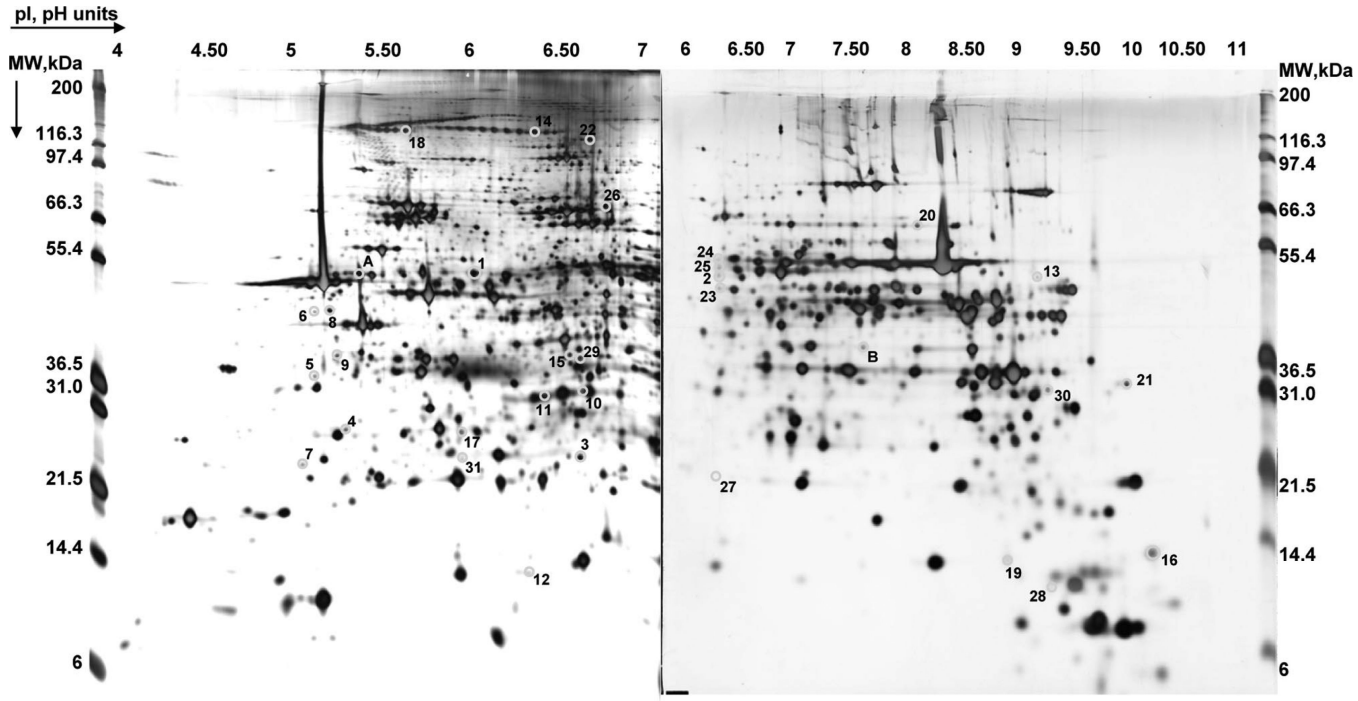

Figure 1.

Mitochondrial proteome. Representative silver stained 2DE gels on 2 pI ranges: 4 to 7 and 6 to 11. The pI (based on linear distribution) and MW (based on MW markers) values are shown on the top and on the sides, respectively. Proteins are numbered according to Table 2.

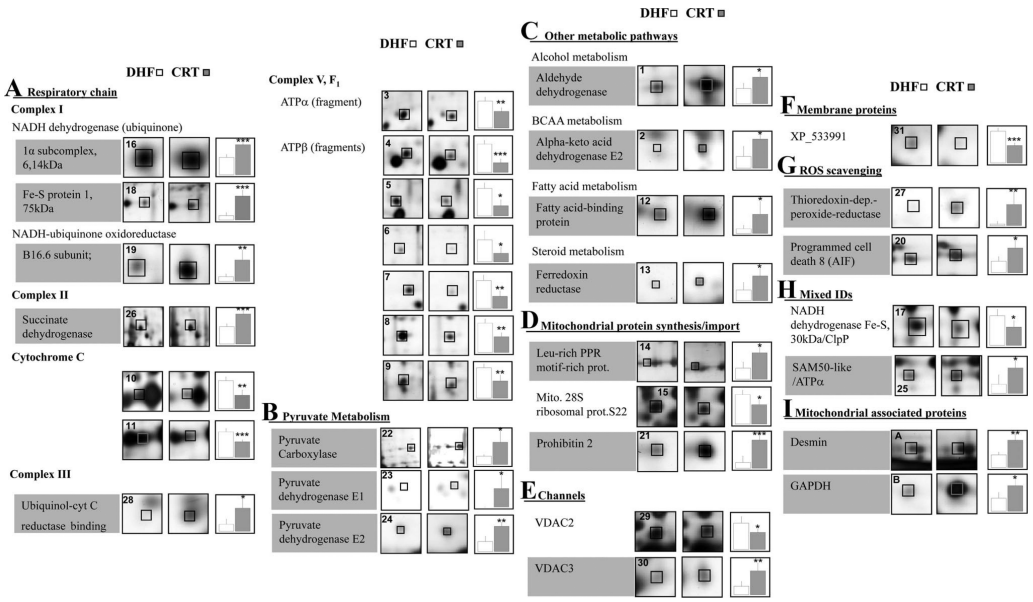

Figure 2.

Protein changes with CRT. Magnified spot images from CRT and DHF representative gels are presented along with plots of their normalized, background subtracted volume. Protein spots are numbered according to Table 2. Protein names with grey backgrounds are those that increased with CRT.

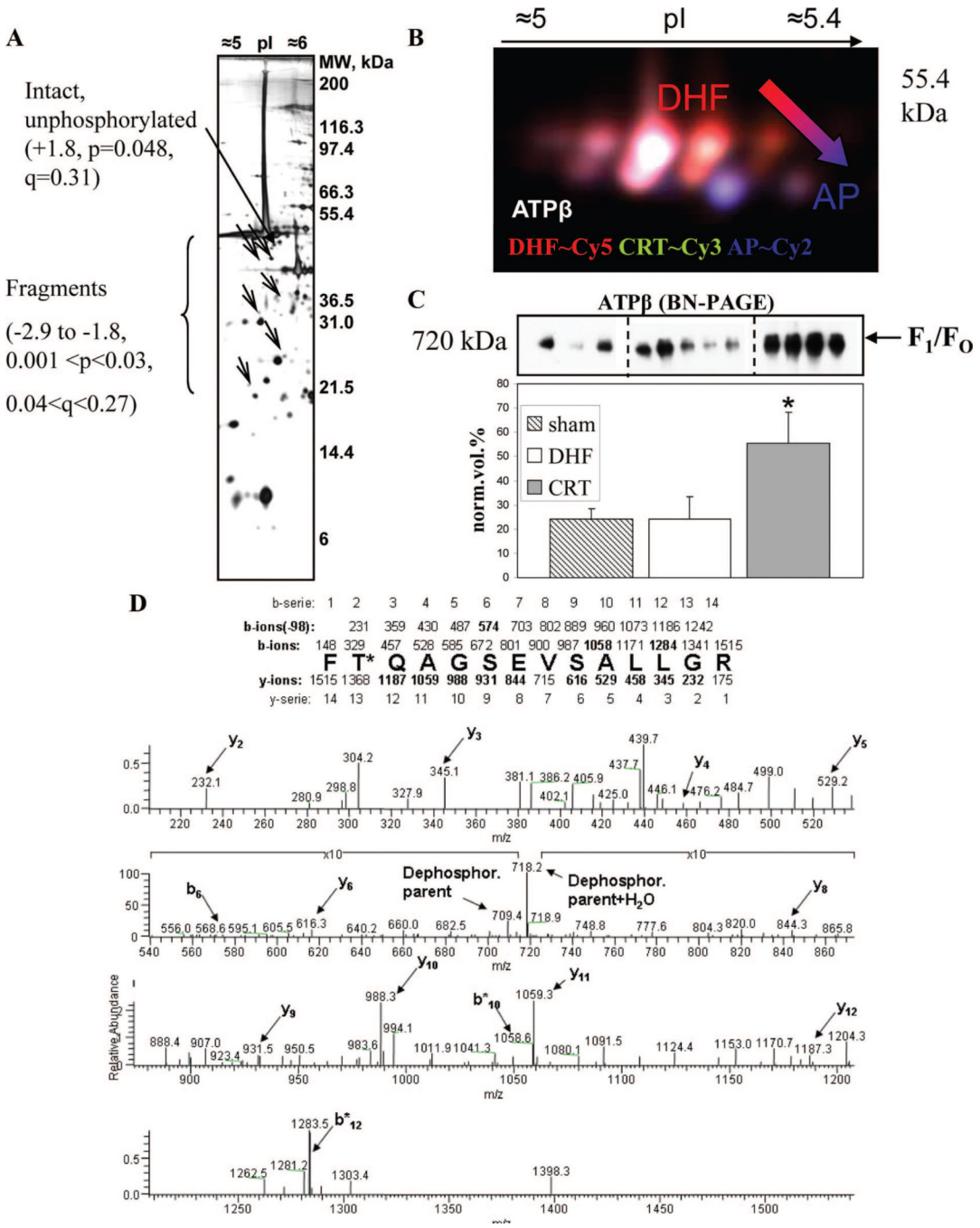

Figure 3.

Characterization of ATP-*β* posttranslational modifications. A, Distribution of changing ATP-*β* on the 2DE gels. The unmodified form (marked with a thicker arrow) and fragments are indicated by arrows and accompanied by fold change values. B, Representative dephosphorylation gel for ATP-*β*. DHF is shown in red (Cy5), CRT in green (Cy3), and the AP-treated pool (AP) in blue (Cy2). C, Representative BN-PAGE/Western blot for ATP-*β*. Biological replicates are shown (3 sham-operated controls, 5 DHF, and 4 CRT). D, Typical MS/MS profile for the phosphopeptide FT*QAGSEVSALLGR. The MS/MS spectrum is provided, together with a schematic in which the mass values for all b- and y-ions series are reported.

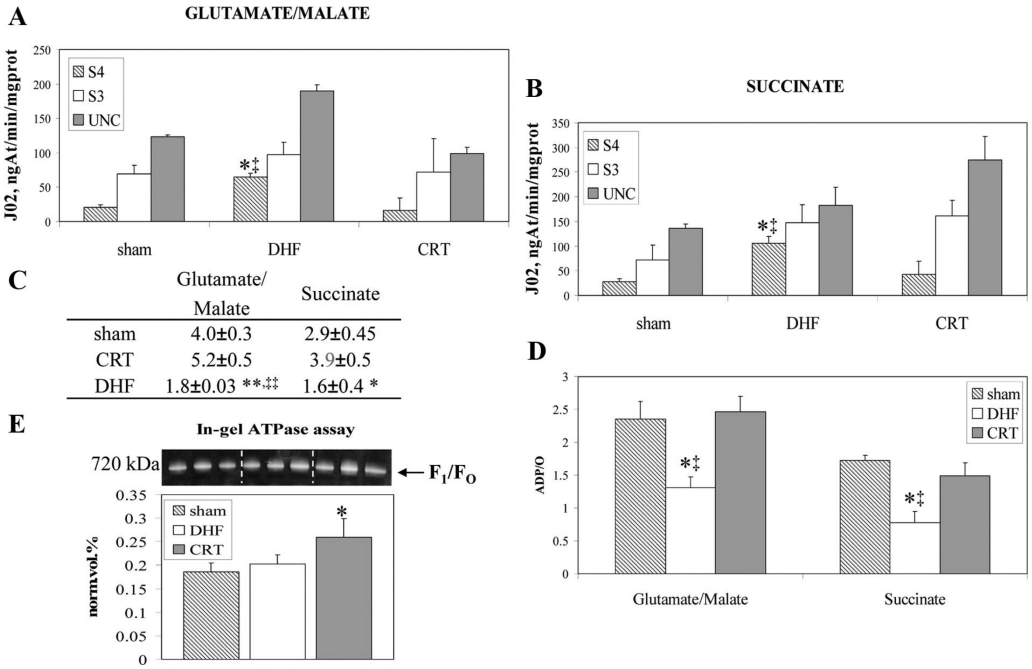

Figure 4.

Mitochondrial bioenergetic parameters. Mitochondrial oxygen consumption was measured in the presence of glutamate/ malate (A) and succinate (B) as substrates. Respiration was monitored in basal state, or state 4 (S4); state 3 (S3), induced by the addition of 300 μM ADP; and uncoupled state, induced by the addition of protonophore 2,4-dinitrophenol (10 μM, uncoupled state). C, Respiratory control ratios. D, ADP/oxygen ratios (**P*<0.05, ***P*<0.001 vs CRT, ‡*P*<0.05, and ‡‡*P*<0.005 vs shams). E, Representative image of the in-gel ATPase assay (n=3). Specific activity is reported as the density of white $PbHPO_4$ bands (product) normalized for the amount of complex V as indicated by coomassie blue G250 stain (**P*=0.02 vs shams and *P*=0.05 vs DHF).

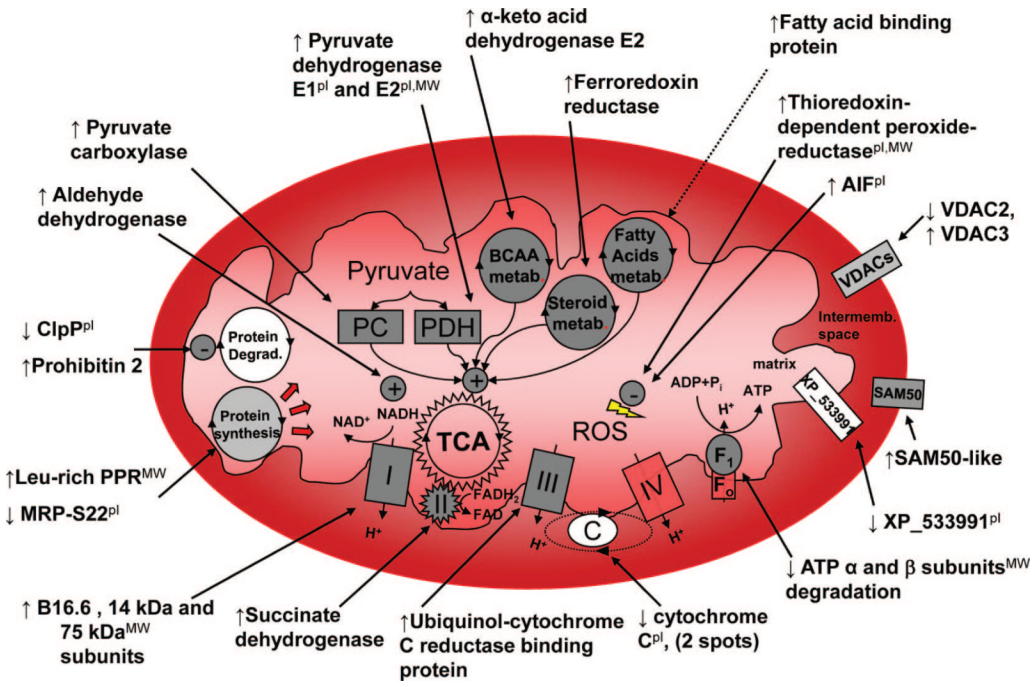

Figure 5.

Schema of mitochondrial protein changes with CRT. For values, refer to Table 2. The pI indicates observed pI differs >1pH unit from predicted one; MW, observed MW differs more than 10 kDa from predicted one. FAD indicates flavin-adenine dinucleotide; $FADH_2$, flavin-adenine dinucleotide, reduced form; NAD^+, oxidized nicotinamide-adenine dinucleotide; P_i, inorganic phosphate; and TCA, tricarboxylic acid. See Table 2 for other abbreviations.

Table 1

Functional Measures of the Canine Model

	DHF	CRT	KW test
Dyssynchrony Index, td	68±4.6	31.3±5.1	<0.0001
Ejection fraction, %	24.8±2.6	33.1±2.6	<0.02
Stroke volume, mL	21.5±2.4	31.9±3.8	<0.02
dP/dtmax/IP, s^{-1})	13.2±0.6	16.9±1.2	<0.02

Kruskal-Wallis (KW).

Table 2

Protein Spots Identifications and Fold Changes

MS/MS ID	SSN	NCBI Account Number	Unique Peptides	Corrected Mowse	Observed, pI/MW	Theoretical, pI/MW	CRT vs DHF	*P*	*q*
Aldehyde dehydrogenase	1	gi 73995214	14	1142	6.0/50	6.63/57	1.7	0.037	0.28
α-Keto acid dehydrogenase E2	2	gi 57088195	10	685	6.3/50	8.46/54	2.5	0.015	0.20
ATP synthase-α (fragment)	3	gi 94574274	13	1203	6.6/24	9.21/60	–1.6	0.006	0.15
ATP synthase-β (fragment)	4	gi 73968432	12	925	5.3/28	5.21/56	–2.9	0.001	0.04
ATP synthase-β (fragment)	5	gi 73968432	14	1224	5.1/36	5.21/56	–2.7	0.010	0.18
ATP synthase-β (fragment)	6	gi 73968432	15	1304	5.1/48	5.21/56	–2.6	0.033	0.27
ATP synthase-β (fragment)	7	gi 73968432	5	422	5.1/23	5.21/56	–2.3	0.004	0.11
ATP synthase-β (fragment)	8	gi 73968432	18	1524	5.2/50	5.21/56	–1.9	0.001	0.08
ATP synthase-β (fragment)	9	gi 73968432	14	1130	5.2/39	5.21/56	–1.8	0.005	0.13
Cytochrome C	10	gi 73974739	9	691	6.6/35	8.8/37	–2.1	0.002	0.08
Cytochrome C	11	gi 73974739	8	610	6.4/35	8.8/37	–1.6	0.001	0.07
Fatty acid-binding protein	12	gi 57043188	5	413	6.3/13	6.29/15	4.2	0.041	0.30
Ferredoxin reductase	13	gi 73964937	5	292	9.0/50	9.37/54	2.3	0.029	0.26
Leucine-rich PPR motif-containing protein (Leu-rich PPR)	14	gi 73970116	24	1595	6.3/131	6.46/158	2.4	0.012	0.19
Mito Ribo S22 (MRP-S22)	15	gi 73990290	15	1082	6.5/40	7.7/41	–1.5	0.013	0.19
NADH-dehydrogenase, 14 kDa	16	gi 73969393	6	457	10.0/13	10.93/23	1.7	0.001	0.04
NADH-dehydrogenase Fe-S 30 kDa	17	gi 73983298	8	666	5.9/28	6.99/30	–1.6	0.031	0.27
NADH-dehydrogenase Fe-S 75 kDa	18	gi 74005216	14	1024	5.7/133	5.85/80	5.5	0.001	0.04
NADH-ubiquinone oxidoreductase B16.6	19	gi 57101296	11	814	8.75/13	8.89/17	4.7	0.007	0.15
Programmed cell death 8 isoform 2 isoform 6 (AIF)	20	gi 74008419	16	1198	8.0/61	9.09/66	2.1	0.022	0.23
Prohibitin 2	21	gi 76616402	12	936	9.7/31	10.04/32	4.8	0.001	0.07
PC	22	gi 73982897	31	2303	6.7/120	6.32/129	2.7	0.033	0.27
PDH E1	23	gi 76660371	10	696	6.3/48	8.54/40	>10	0.035	0.27
PDH E2	24	gi 73954761	3	182	6.4/55	8.39/69	2.5	0.002	0.08
SAM50-like protein CGI-51	25	gi 73969335	12	768	6.3/51	6.44/50	2.8	0.024	0.24
Succinate dehydrogenase	26	gi 74003064	19	1366	6.75/70	7.29/73	2.3	0.001	0.04
Thioredoxin-dependent peroxide reductase	27	gi 73998671	10	765	6.3/20	8.33/28	>10	0.011	0.19

Circ Cardiovasc Genet. Author manuscript; available in PMC 2010 August 16.

MS/MS ID	SSN	NCBI Account Number	Unique Peptides	Corrected Mowse	Observed, pI/MW	Theoretical, pI/MW	CRT vs DHF	*P*	*q*
Ubiquinol-cytochrome C reductase binding protein	28	gi 73999619	9	566	9.2/11	9.10/17	3.3	0.013	0.20
VDAC2	29	gi 73953097	9	776	6.6/39	7.48/32	–1.6	0.036	0.28
VDAC3	30	gi 73979119	8	735	9.0/30	8.95/31	2.8	0.007	0.15
XP_533991	31	gi 73987821	10	636	5.9/24	6.99/30	–1.8	0.001	0.04
Mitochondria associated proteins									
Desmin	A	gi 59958381	28	2063	5.3/53	5.21/53	2.1	0.003	0.10
GAPDH	B	gi 50978862	7	504	7.6/38	6.90/36	2.0	0.023	0.23

Two levels of stringency were applied for both statistical ($P \leq 0.05$, $q \leq 0.3$, or 30% false discovery rate) and biological (1.5-fold change) significance. Proteins with $q > 0.2$, which normally would not merit claims of signals were retained for their "biological coherence" (eg, subunits of the same complex, see the online Data Supplement). AIF indicates apoptosis-inducing factor; GAPDH, glyceraldehyde 3-phosphate dehydrogenase; NADH, reduced nicotinamide-adenine dinucleotide; PC, pyruvate carboxylase; PDH, pyruvate dehydrogenase; PPR; and VDAC, voltage-dependent anion channel.

Circ Cardiovasc Genet. Author manuscript; available in PMC 2010 August 16.